Available online at www.sciencedirect.com
SCIENCE DIRECT®
Bioorganic & Medicinal Chemistry 13 (2005) 2045–2053
Bioorganic & Medicinal Chemistry

Synthesis, conformational analysis, and biological activity of new analogues of thiazole-4-carboxamide adenine dinucleotide (TAD) as IMP dehydrogenase inhibitors

Palmarisa Franchetti,[a] Loredana Cappellacci,[a] Michela Pasqualini,[a] Riccardo Petrelli,[a] Vetrichelvan Jayaprakasan,[b] Hiremagalur N. Jayaram,[b] Donald B. Boyd,[c] Manojkumar D. Jain[d] and Mario Grifantini[a,*]

[a]*Dipartimento di Scienze Chimiche, Università di Camerino, 62032 Camerino, Italy*
[b]*Department of Biochemistry and Molecular Biology, and Richard Roudebush Veterans Affairs Medical Center, Indiana University School of Medicine, Indianapolis, IN 46202, USA*
[c]*Department of Chemistry, Indiana University–Purdue University at Indianapolis, IN 46202, USA*
[d]*School of Informatics, Indiana University–Purdue University at Indianapolis, IN 46202, USA*

Received 16 November 2004; revised 28 December 2004; accepted 7 January 2005
Available online 23 January 2005

Abstract—Thiazole-4-carboxamide adenine dinucleotide (TAD) analogues T-2′-MeAD (**1**) and T-3′-MeAD (**2**) containing, respectively, a methyl group at the ribose 2′-*C*-, and 3′-*C*-position of the adenosine moiety, were prepared as potential selective human inosine monophosphate dehydrogenase (IMPDH) type II inhibitors. The synthesis of heterodinucleotides was carried out by CDI-catalyzed coupling reaction of unprotected 2′-*C*-methyl- or 3′-*C*-methyl-adenosine 5′-monophosphate with 2′,3′-*O*-isopropylidene-tiazofurin 5′-monophosphate, and then deisopropylidenation. Biological evaluation of dinucleotides **1** and **2** as inhibitors of recombinant human IMPDH type I and type II resulted in a good activity. Inhibition of both isoenzymes by T-2′-MeAD and T-3′-MeAD was noncompetitive with respect to NAD substrate. Binding of T-3′-MeAD was comparable to that of parent compound TAD, while T-2′-MeAD proved to be a weaker inhibitor. However, no significant difference was found in inhibition of the IMPDH isoenzymes. T-2′-MeAD and T-3′-MeAD were found to inhibit the growth of K562 cells (IC_{50} 30.7 and 65.0 μM, respectively).

1. Introduction

Nucleotide coenzymes participate in essential enzyme-catalyzed redox reactions and play a fundamental role in cellular metabolic processes such as nicotinamide adenine dinucleotide (NAD) in the case of dehydrogenases. It has been shown that in many living organisms, disturbance of the nucleotide metabolism causes severe consequences for cell survival. Altered NAD metabolism has been observed in many cancers. Some NAD analogues modified at the nicotinamide moiety have been identified as active metabolites of nucleosides endowed with antitumor and antiviral potency. These dinucleotides are potent inhibitors of inosine 5′-monophosphate dehydrogenase (IMPDH), a rate-limiting enzyme of de novo guanine nucleotides biosynthesis. IMPDH, which catalyzes the NAD-dependent conversion of inosine 5′-monophosphate (IMP) to xanthosine 5′-monophosphate (XMP), was shown to be significantly increased in highly proliferative cells. Inhibition of this enzyme results in a decrease in GTP and dGTP biosynthesis, producing inhibition of tumor cell proliferation.[1] It was found that IMPDH exists in two isoforms, type I and type II, which are regulated differently. While type I is constitutively expressed, type II is up-regulated and predominates in neoplastic and fast replicating cells.[2–4] Thus, the selective inhibition of IMPDH type II may provide improved selectivity against target cells in anticancer chemotherapy.

Some *C*-nucleosides such as the antitumor drug tiazofurin and the analogue selenazofurin are metabolized in tumor cells sensitive to these agents to their

Keywords: TAD analogues; IMPDH inhibitors; Cytotoxicity.
* Corresponding author. Tel.: +39 0737 402233; fax: +39 0737 637345; e-mail: mario.grifantini@unicam.it

0968-0896/$ - see front matter © 2005 Elsevier Ltd. All rights reserved.
doi:10.1016/j.bmc.2005.01.007

corresponding thiazole-4-carboxamide- and selenazole-4-carboxamide-adenine dinucleotides (TAD and SAD, respectively).[5,6] These dinucleotides, which resulted to be potent noncompetitive inhibitors of IMPDH, bind to the NAD active site of the enzyme. Nevertheless, TAD, SAD, or other analogues did not show significant isoform specificity[7] (Fig. 1).

Crystallographic studies of human type II IMPDH complexed with SAD have shown that the dinucleotide is stacked between the aromatic residues His 253 and Phe 282, while forming with the adenine moiety an edge-on interaction with Thr 252, as well as with Thr 45 from the adjacent monomer of the tetrameric protein.[8] Three of these residues are not conserved between the type I and type II isoforms: His 253(II) → Arg(I), Phe 282(II) → Tyr(I), and Thr 45(II) → Ile(I). Thus, we conjectured that ligand modification in the dinucleotide adenosine moiety may provide some degree of isoform specificity. It should be noted that the structure of a dinucleotide and the conformation around the glycosidic bond that determines the orientation of the heterocyclic substituent relative to the ribose ring, are determinant factors in the drug–enzyme interaction. In fact, any chemical modification of the nucleotide undoubtedly alters these parameters.

In order to investigate the subdomain that binds the adenosine moiety of TAD, we have synthesized two new dinucleotide analogues in which the ribofuranose moiety of adenosine was replaced by 2-*C*-methyl ribose (T-2′-MeAD, **1**) or 3-*C*-methyl ribose (T-3′-MeAD, **2**), and studied their conformation in relation to the inhibitory activity against the human IMPDH isoforms.

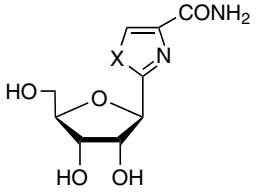

Tiazofurin (X = S)
Selenazofurin (X = Se)

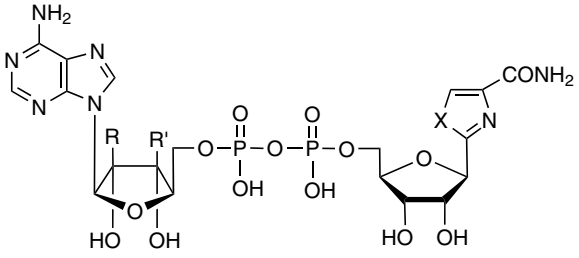

TAD (R = R' = H, X = S)
SAD (R = R' = H, X = Se)
T-2'-MeAD (R = CH_3, R' = H, X = S)
T-3'-MeAD (R = H, R' = CH_3, X = S)

Figure 1.

2. Results and discussion

2.1. Chemistry

The synthesis of T-2′-MeAD (**1**) and T-3′-MeAD (**2**) as reported in Scheme 1, was performed by coupling of the 2′-*C*-methyladenosine and 3′-*C*-methyladenosine 5′-monophosphates (2′-MeAMP (**5**) and 3′-MeAMP (**7**), respectively) as imidazolide derivatives (**6** and **8**, respectively) with the mono *n*-tributylammonium salt of 2′,3′-*O*-isopropylidene-tiazofurin 5′-monophosphate (**9**). 2′-MeAMP (**5**), previously reported by Ong et al.[9] was prepared by direct phosphorylation of unprotected 2′-*C*-methyladenosine[10] (**3**) with phosphoryl chloride in anhydrous trimethyl phosphate. 3′-MeAMP (**7**) was synthesized from **4** as reported by Ong et al.[11] In these reactions, 2′-*O*-, or 3′-*O*-, or 2′,3′-*O*-phosphorylated derivatives were not detected. Monophosphates **5** and **7** were activated as imidazolides with an excess of 1,1′-carbonyldiimidazole (CDI) in quantitative yield. The CDI activation of **5** and **7** was monitored by TLC and ^{31}P NMR (D_2O) and intermediates **6** and **8** required no isolation. Compound **9** was obtained from acetonide-protected tiazofurin that was synthesized by the Gebeyehu et al. procedure.[12] Phosphorylation of 2′,3′-*O*-isopropylidene-tiazofurin was performed as reported for **5** obtaining the pure nucleotide by a different manner of purification with respect to that reported by Zatorski et al.[13] The coupling reaction was performed in dry DMF at 30 °C for 10 days affording the heterodinucleotides **10** and **11**, which were purified on a silica gel column separating the unreacted mononucleotide **5** or **7** and **9** in small amount. In these reactions, the homodinucleotides of both 2′-*C*-methyl- and 3′-*C*-methyladenosine [P^1,P^2-bis(2′-*C*-methyladenosine-5′-yl)pyrophosphate (**12**), and P^1,P^2-bis(3′-*C*-methyladenosine-5′-yl)pyrophosphate (**13**)] were also obtained (6% and 5%, respectively). At first, we used the acetonide monophosphate derivatives of nucleosides **3** and **4** for the CDI activation. However, the subsequent coupling reaction with **9** proceeded with a yield of desired dinucleotides **1** and **2** similar to that of the above described reactions. Deblocking of **10** and **11** by treatment with 90% formic acid and chromatographic purification afforded the pure pyrophosphates **1** and **2** as determined by HPLC. Characterization of these dinucleotides was achieved by high resolution ^{1}H, and ^{31}P NMR spectroscopy and mass spectrometry. Information concerning the predominant solution conformation of these TAD analogues was obtained via ^{1}H NMR experiments by nuclear Overhauser enhancement (NOE) effects in D_2O. A one-dimensional differential NOE experiment with irradiation of methyl protons of 2′-*C*-, or 3′-*C*-methyladenosine moiety of **1** or **2** showed the complete lack of H-2 enhancement in the purine ring supporting a spatial arrangement where H-2 and the protons of methyl group are not proximate, as would be the case in the *anti* conformers. Because of the overlapping of the proton signals in position 3 and 4 of the ribose moieties, it was impossible to determine the sugar puckering of these dinucleotides by ^{1}H NMR experiments. However, we previously found that 2′-*C*-methyladenosine has a marked preference for the North ($^3T_2$) conformation in solution, while 3′-*C*-methyladeno-

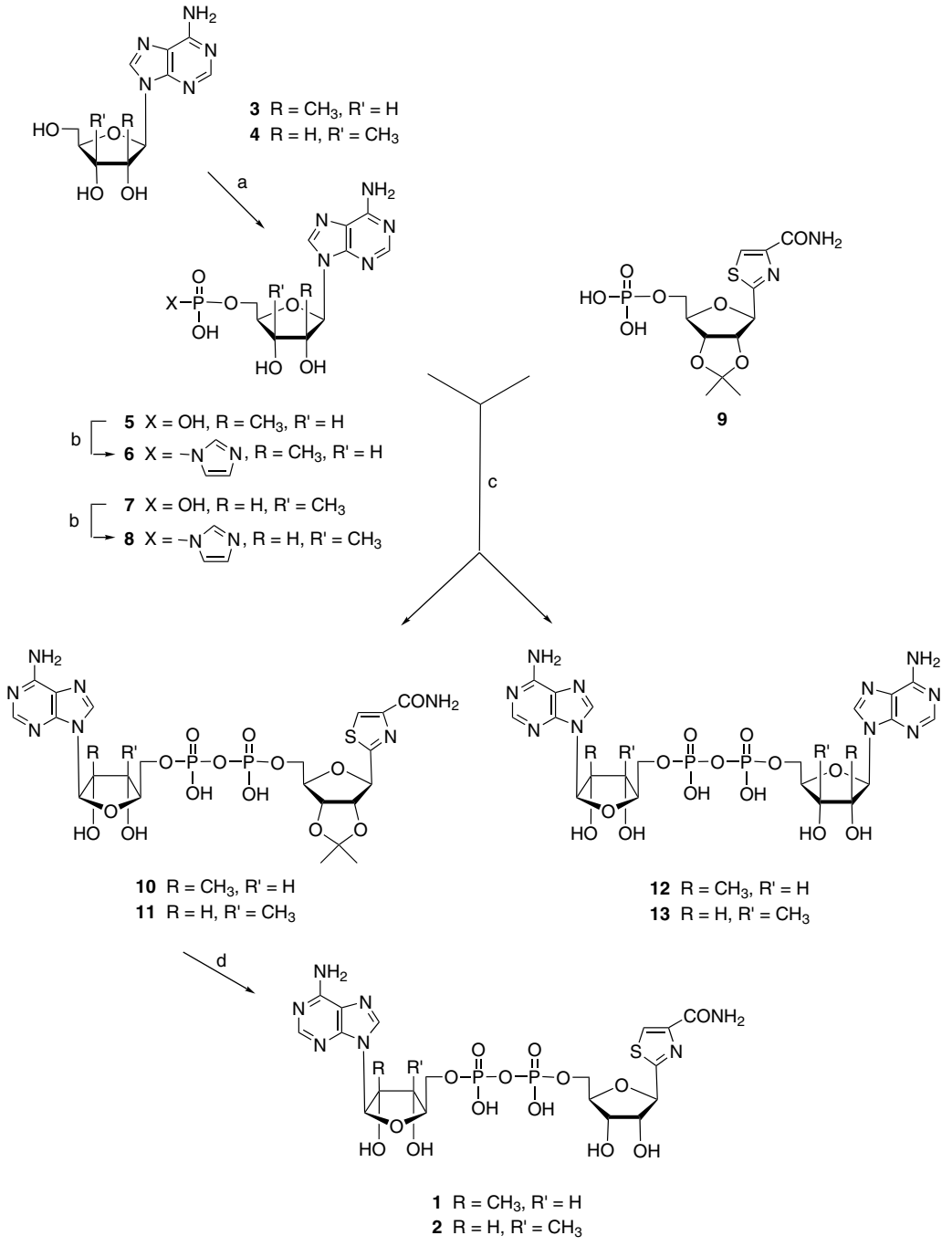

Scheme 1. Reagents and conditions: (a) $POCl_3$, $(MeO)_3PO$, 0 °C; (b) CDI, DMF rt; (c) $(n\text{-Bu})_3N$, DMF 30 °C; (d) 90% HCOOH, rt.

sine showed a preference for the South ($^2T_3$) conformation.[10] Thus, it is likely that the preference of the adenosine moiety for these conformations is maintained in T-2′-MeAD and T-3′-MeAD.

2.2. Molecular modeling

TAD and its methyl analogues **1** and **2** have many rotatable bonds and are therefore highly flexible. This flexibility allows the ligand to adjust its conformation when it binds to the active site in IMPDH. Conversely, most enzymes have some degree of flexibility in the backbone and especially the side chains to accommodate different ligands. However, it is known from the medicinal chemistry that there are cases where adding a methyl group to a drug molecule can significantly decrease bioactivity or change selectivity, so there are limits to how much an enzyme can adapt its shape to achieve affinity to different ligands.[14–16]

We investigated the effect of methylation at the ribose of adenosine moiety on the conformational properties of TAD. We used the standard molecular modeling techniques of energy minimization (to optimize bond lengths, bond angles, torsional angles), conformational searching (to find the most stable conformers), and

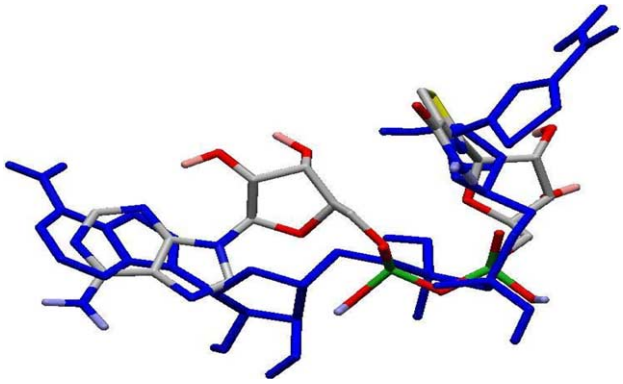

Figure 2. TAD after energy minimization of 1ADF (blue) and TAD after molecular dynamics (multi-color) with water as solvent and then energy minimization using MMFF94s in MACROMODEL. The RMSD is 4.22 Å from the least squares fitting of paired atoms in each molecule.

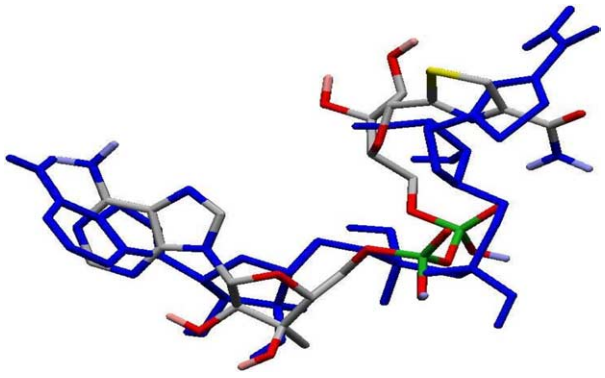

Figure 4. T-3′-MeAD after energy minimization of 1ADF (blue) and T-3′-MeAD after molecular dynamics (multi-color) with water as solvent and then energy minimization using MMFF94s in MACROMODEL. The RMSD is 2.94 Å.

molecular dynamics simulations (to explore the conformational variability of the molecules).[14–16] The molecular mechanics methods detailed in Section 4 were used. One X-ray structure available in the Protein Data Bank (PDB)[17] is alcohol dehydrogenase (E.C.1.1.1.1) complexed with the inhibitor β-methylene-thiazole-4-carboxamide adenine dinucleotide (β-TAD).[18] This crystalline complex is referred to as 1ADF in the PDB. We extracted the atomic coordinates of the TAD ligand, added hydrogens at standard geometries, and assigned appropriate atom and bond types in order to prepare the structure for molecular mechanics calculations. Crystallografically, TAD is observed in an extended conformation, whereas a systematic conformational search indicates the global minimum energy structure is folded. This is typical of molecular mechanics results for gas-phase molecules because of attractive intramolecular van der Waals interactions.[19] Figure 2 compares the structure of TAD before and after molecular mechanics simulations that include the effect of aqueous solvation. Likewise, Figure 3 shows the structure of T-2′-MeAD before and after the simulations in a water environment, and Figure 4 shows the same for T-3′-MeAD. It can be seen in each case that the molecules can explore quite an extensive range of conformational space while maintaining an overall extended conformation.

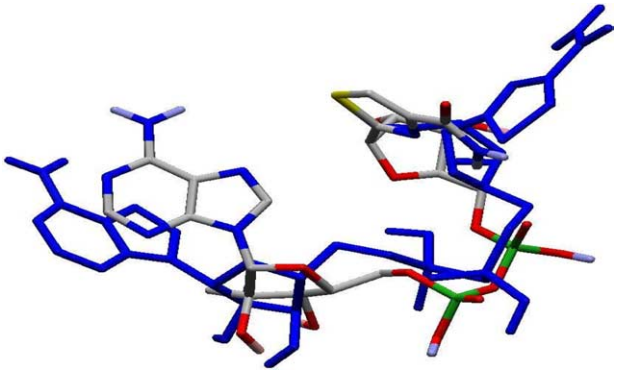

Figure 3. T-2′-MeAD after energy minimization of 1ADF (blue) and T-2′-MeAD after molecular dynamics (multi-color) with water as solvent and then energy minimization using MMFF94s in MACROMODEL. The RMSD is 3.34 Å.

2.3. Biological evaluation

The inhibitory effects of T-2′-MeAD and T-3′-MeAD against recombinant human IMPDH type I and type II, using TAD and tiazofurin as reference compounds, were examined. K_i values of these compounds for each isoform of IMPDH were determined as described in Section 4 (Table 1). All compounds exhibited noncompetitive-type inhibition toward NAD cofactor of both enzymes' isoforms. TAD was the most potent inhibitor showing a similar inhibitory activity against both IMPDH isoforms (type I: K_i toward NAD utilization 0.19 μM; type II: K_i 0.24 μM). T-3′-MeAD was 2.7-fold less potent than TAD with a similar affinity toward IMPDH type I and type II, while T-2′-MeAD proved a weaker inhibitor being about 5-fold less potent than TAD. Tiazofurin was found inactive as IMPDH inhibitor at concentrations up to 1 mM. The higher inhibitory activity of T-3′-MeAD as compared to that of T-2′-MeAD may be explained by the preference of

Table 1. Inhibition of type I and type II human IMPDH and K562 sensitive and tiazofurin resistant cells growth by TAD analogues T-2′-MeAD and T-3′-MeAD

Compound	Inhibition K_i (μM)[a]		K562/S cytotoxicity IC_{50} (μM)[b]	K562/TR cytotoxicity IC_{50} (μM)[b]
	IMPDH-I	IMPDH-II		
T-2′-MeAD	1.10	1.14	65.0	na[c]
T-3′-MeAD	0.52	0.66	30.7	223.3
TAD	0.19	0.24	8.9	1230
Tiazofurin	—	—	4.5	1230

[a] Saturated concentrations (100 μM) of both substrates (IMP and NAD) were used. The pattern of inhibition in each case is noncompetitive.

[b] Concentration required to inhibit 50% of cell proliferation at 48 h. Values were obtained at 37 °C.

[c] No inhibition was observed up to a concentration of 167 μM.

the first dinucleotide for a conformation of the adenosine moiety very close to that of TAD, as shown in Figure 2. We found that O5′–C1′–N9–C4 dihedral angles for adenosine moiety in the minimized structures of TAD and T-3′-MeAD are essentially the same (173°), while the dihedral angle for T-2′-MeAD was higher (179°).

T-2′-MeAD and T-3′-MeAD were also tested for their cytotoxicity against human myelogenous leukemia K562 in culture using TAD and tiazofurin as reference compounds (Table 1). The most active compounds proved to be tiazofurin and TAD with IC_{50} values of 4.5 and 8.9 μM, respectively, while T-2′-MeAD and T-3′-MeAD were found to be less cytotoxic (IC_{50} values of 65.0 and 30.7 μM, respectively). T-3′-MeAD was found to be active, although to a lesser degree, against K562 cells resistant to tiazofurin. In this case TAD, T-2′-MeAD and tiazofurin proved to be very little active or inactive.

It is worth noting that the tested dinucleotides, being charged molecules, have difficulty in crossing cell membranes, so their cytotoxicity is likely related to their ability to undergo prior hydrolysis in the culture medium, followed by reassembly within the cell. We have verified this hypothesis by evaluating the stability to enzymatic degradation of both TAD analogues in RPMI-1640 medium containing 10% fetal calf serum at 37 °C (pH 7.3). Under these conditions both dinucleotides **1** and **2** were broken down into 5′-monophosphates, and then into free nucleosides, tiazofurin and 2′-*C*-methyl- and 3′-*C*-methyladenosine, respectively, with a $t_{1/2}$ of 3.2 h (T-2′-MeAD), and 5.5 h (T-3′-MeAD). The activity of T-3′-MeAD against tiazofurin resistant K562 cells could be ascribed in part to 3′-*C*-methyladenosine, that proved to be active with an IC_{50} value of 38.3 μM.[20] In this type of cells 2′-*C*-methyladenosine was devoid of activity.

3. Conclusions

In summary, we have further investigated the structural conformations of TAD, the active anabolite of the antitumor drug tiazofurin, targeted to inhibit IMPDH in hope of obtaining selective inhibitors of IMPDH type II, the predominant isoform in neoplastic cells. The adenosine portion of TAD was modified in the ribose moiety to influence the conformation and binding at the active sites of the enzyme by structural differences with respect to dinucleotide congener. The 2′-*C*-, or 3′-*C*-methyl-modification in the dinucleotide pyrophosphates T-2′MeAD and T-3′-MeAD resulted in stabilization of the North ($^3T_2$) or South ($^2T_3$) conformation of the sugar, respectively. This causes a decrease of the inhibitory activity of the dinucleotides against both types of recombinant IMPDH isoforms with respect to TAD. It should be noted that, while the adenosine ribose prefers the 3′-*endo* pucker in solution, the adenosine ribose of TAD shows 2′-*endo* pucker [South ($^2T_3$) conformation],[18] similar to that of T-3′-MeAD, and different to that of T-2′-MeAD (3′-*endo*). This might explain the correlation of the structural difference of these dinucleotides with the difference in enzymatic activity when compared to the dinucleotide congener. The decrease in activity is more remarkable in the case of the 2′-*C*-substitution in TAD (T-2′-MeAD). It appears that the variation of conformation of the adenosine moiety in T-2′-MeAD and T-3′-MeAD impairs the ability of 2′- and 3′-hydroxy group of the ribose and/or the purine moiety to bind the NAD site of both IMPDH isoforms.

4. Experimental

4.1. Chemistry

4.1.1. General procedure. All reagent and solvents were purchased from Aldrich Chemical Co. The analytical samples of nucleotides were lyophilized or dried in vacuo over P_2O_5. Thin layer chromatography (TLC) was run on silica gel 60 F_{254} plates; silica gel 60 (70–230 mesh, Merck) for column chromatography was used. HPLC was performed on an Ultrasphere (Beckman) RP18 column for evaluation of the T-2′-MeAD purity with flow rate of 1 mL/min of MeCN–H_2O (6:4, v/v). For T-3′-MeAD, a LiChroCART 125-3 (Merck) RP18 endcapped (5 mm) Purospher column with flow rate of 0.8 mL/min of buffer A (100 mM KH_2PO_4) 95%, and buffer B (100 mM KH_2PO_4 in 20% MeOH) 5% was used. Nuclear magnetic resonance spectra were recorded on a Varian VXR-300 spectrometer with TMS as the internal standard for ^1H NMR and external H_3PO_4 for ^{31}P NMR. Chemical shift are reported in part per million (δ) as s (singlet), d (doublet), t (triplet), dd (double doublet), q (quartet), m (multiplet), or br s (broad singlet). Stationary NOE experiments were run on degassed solutions at 25 °C. Mass spectroscopy was carried out on an HP 1100 series instrument. All measurements were performed in the negative ion mode using an atmospheric pressure electrospray ionization (API-ESI). Tiazofurin was obtained through the Drug Synthesis and Chemistry Branch, National Cancer Institute (Bethesda). TAD was prepared according to the literature procedure.[12]

4.1.2. 9*H*-(2′-*C*-Methyl-β-D-ribofuranosyl)adenine-5′-monophosphate (5).[11] To a cooled mixture of **3**[10] (180 mg, 0.56 mmol) and $(CH_3O)_3PO$ (3.5 mL) was added $POCl_3$ dropwise (0.11 mL, 1.87 mmol) and the mixture was kept at 0 °C for 17 h. After neutralization with 1 N NaOH, the solution was washed with $CHCl_3$ (3 × 10 mL). Concentration of the aqueous layer in vacuo gave a residue, which was purified by chromatography on a DEAE Sephadex (HCO_3^- form) column eluting with a linear gradient of H_2O and 0.5 M NH_4HCO_3. Compound **5** was converted into free acid form by passing it through a Dowex 50-X8 (H^+) column eluting with H_2O and dried in vacuo in the presence of P_2O_5 overnight (amorphous solid, 165 mg, 66% yield). ^1H NMR (D_2O): δ 0.9 (s, 3H, CH_3), 4.10–4.30 (m, 4H, H3′, H4′, H5′), 6.15 (s, 1H, H1′), 8.35 (s, 1H, H2), 8.55 (s, 1H, H8). ^{31}P NMR (D_2O): δ 0.79 (br s). MS *m/z* 360.2 $[MH]^-$. Anal. ($C_{11}H_{16}N_5O_7P{\cdot}H_2O$) C, H, N.

4.1.3. 2-(2′,3′-*O*-Isopropylidene-5′-monophosphate-β-D-ribofuranosyl)thiazole-4-carboxamide (9).[13] The title compound was synthesized starting from 2-(2′,3′-*O*-isopropylidene-β-D-ribofuranosyl)thiazole-4-carboxamide[12] as reported for **5** (reaction time 2 h). Compound **9** was obtained as a free acid (white amorphous solid, 70% yield). ^{1}H NMR (D_2O): δ 1.35, 1.55 (2s, 6H, $(CH_3)_2C$), 3.75 (m, 2H, H5′), 4.40 (m, 1H, H4′), 4.90 (dd, J = 2.6, 6.3 Hz, 1H, H3′), 5.04 (dd, J = 4.3, 6.4 Hz, 1H, H2′), 5.26 (d, J = 4.3 Hz, 1H, H1′), 8.18 (s, 1H, H5). ^{31}P NMR (D_2O): δ 0.70 (br s). MS m/z 339.0 $[MH]^-$. Anal. ($C_{12}H_{17}N_2O_8PS\cdot H_2O$) C, H, N.

4.1.4. P^1-5′-[2-(2′,3′-*O*-isopropylidene-β-D-ribofuranosyl)thiazole-4-carboxamide]-P^2-5′-[6-amino-9*H*-(2′-*C*-methyl-β-D-ribofuranosyl)purine]pyrophosphate (10). Compound **5** (160 mg, 0.49 mmol) was coevaporated with dry DMF (2 × 2 mL) and then was dissolved in dry DMF (3 mL). 1,1′-Carbonyldiimidazole (291 mg, 1.8 mmol) was added and the reaction was monitored by TLC (*i*-PrOH/NH_4OH/H_2O, 70:20:10) and by ^{31}P NMR (D_2O, −3.5 ppm for compound **6**). After 4 h, dry MeOH (117 mL) was added to hydrolyze excess CDI stirring for 30 min. To imidazolide **6**, a solution of **9** (230 mg, 0.54 mmol) in dry DMF (2 mL) containing Bu_3N (128 mL, 0.54 mmol) was added and the mixture was kept at 30 °C for 10 days. After that time, H_2O (14 mL) was added and the solution was extracted with $CHCl_3$ (2 × 10 mL) and Et_2O (2 × 10 mL). The aqueous phase was concentrated to dryness and the residue was applied on a silica gel column eluting with *i*-PrOH/NH_4OH/H_2O (85:10:5) to give **10** as a white foam (diammonium salt, 86 mg, 30% yield). ^{1}H NMR (D_2O): δ 1.05 (s, 3H, CH_3), 1.25, 1.50 (2s, 6H, $(CH_3)_2C$), 3.90 (m, 2H, H5′(2′-Me-A)), 4.10 (m, 2H, H5′(T)), 4.30 (m, 2H, H4′(2′-Me-A), H4′(T)), 4.40 (m, 1H, H3′(2′-Me-A)), 4.80 (m, 2H, H2′(T), H3′(T)), 5.0 (d, J = 4.3 Hz, 1H, H1′(T)), 6.15 (s, 1H, H1′(2′-Me-A)), 8.03 (s, 1H, H5(T)), 8.32 (s, 1H, H2(2′-Me-A)), 8.43 (s, 1H, H8(2′-Me-A)). ^{31}P NMR (D_2O): δ −10.8 (br s). MS m/z 722.2 $[MH]^-$. Anal. ($C_{23}H_{37}N_9O_{14}P_2S\cdot 2H_2O$) C, H, N.

From the same column, the starting compounds **5** (7%) and **9** (4%) were separated. P^1,P^2-bis(2′-*C*-methyladenosine-5′-yl)pyrophosphate (**12**) as a white foam was also separated (6%). ^{1}H NMR (D_2O): δ 0.65 (s, 3H, CH_3), 4.0–4.20 (m, 8H, H3′, H4′, H5′), 5.72 (s, 2H, H1′), 7.85 (s, 2H, H2), 8.08 (s, 2H, H8). ^{31}P NMR (D_2O): δ −10.75 (br s). MS m/z 703.2 $[MH]^-$. Anal. ($C_{22}H_{36}N_{12}O_{13}P_2\cdot 2H_2O$) C, H, N.

4.1.5. P^1-5′-[2-(β-D-ribofuranosyl)thiazole-4-carboxamide]-P^2-5′-[6-amino-9*H*-(2′-*C*-methyl-β-D-ribofuranosyl)purine]pyrophosphate (1). Compound **10** (80 mg, 0.1 mmol) was treated with 90% HCOOH (1.8 mL) and stirred at room temperature for 5 h. The solution was concentrated in vacuo and coevaporated with dry MeOH (5 × 5 mL). The crude residue was purified by chromatography on a silica gel column eluting with *i*-PrOH/NH_4OH/H_2O (75:20:5) to give **1** as a white foam that was lyophilized (diammonium salt, 53 mg, 75% yield). The purity of **1** by analytical HPLC was 98% (t_R = 7.1 min). ^{1}H NMR (D_2O): δ 0.85 (s, 3H, CH_3), 4.05–4.38 (m, 8H, H5′(T), H5′(2′-Me-A), H4′(2′-Me-A), H4′(T), H3′(2′-Me-A), H3′(T)), 4.40 (m, 1H, H2′(T)), 4.92 (d, J = 5.5 Hz, 1H, H1′(T)), 6.02 (s, 1H, H1′(2′-Me-A)), 7.92 (s, 1H, H5(T)), 8.12 (s, 1H, H2(2′-Me-A)), 8.35 (s, 1H, H8 (2′-Me-A)). ^{31}P NMR (D_2O): δ −10.7 (br s). MS m/z 682.2 $[MH]^-$. Anal. ($C_{20}H_{33}N_9O_{14}P_2S\cdot 3H_2O$) C, H, N.

4.1.6. 6-Amino-9*H*-(3′-*C*-methyl-β-D-ribofuranosyl)-purine-5′-monophosphate (7).[11] This compound was prepared as described for **5** starting from **4** (457 mg, 1.65 mmol) as an amorphous solid (reaction time 12 h, 63% yield). ^{1}H NMR (D_2O): δ 1.35 (s, 3H, CH_3), 3.92 (pseudo t, 2H, H5′), 4.20 (pseudo q, 1H, H4′), 4.50 (d, J = 7.9 Hz, 1H, H2′), 6.02 (d, J = 7.6 Hz, 1H, H1′), 8.22 (s, 1H, H2), 8.55 (s, 1H, H8). ^{31}P NMR (D_2O): δ 0.25 (s). MS m/z 360.2 $[MH]^-$. Anal. ($C_{11}H_{16}N_5O_7P\cdot H_2O$) C, H, N.

4.1.7. P^1-5′-[2-(2′,3′-*O*-isopropylidene-β-D-ribofuranosyl)thiazole-4-carboxamide]-P^2-5′-[6-amino-9*H*-(3′-*C*-methyl-β-D-ribofuranosyl)purine]pyrophosphate (11). This compound was prepared as reported for **10** starting from **7** (356 mg, 0.87 mmol) through imidazolide **8** (reaction time 7 days). Chromatography on a silica gel column eluting with *i*-PrOH/NH_4OH/H_2O (77:13:10) gave **11** as a white foam (diammonium salt, 132 mg, 21% yield). ^{1}H NMR (D_2O): δ 1.25, 1.50 (s, 6H, $(CH_3)_2C$), 1.38 (s, 3H, CH_3), 3.90 (m, 2H, H5′(3′-Me-A)), 4.10 (m, 2H, H5′(T)), 4.22 (m, 1H, H4′(3′-Me-A)), 4.30 (m, 1H, H4′(T)), 4.78 (m, 2H, H2′(T), H3′(T)), 5.0 (d, J = 4.0 Hz, 1H, H1′(T)), 5.35 (d, J = 7.6 Hz, 1H, H2′(3′-Me-A)), 6.10 (d, J = 8.3 Hz, 1H, H1′(3′-Me-A)), 7.90 (s, 1H, H5(T)), 8.02 (s, 1H, H8(3′-Me-A)), 8.40 (s, 1H, H2(3′-Me-A)). ^{31}P NMR (D_2O): δ −11.2 (br s). MS m/z 722.2 $[MH]^-$. Anal. ($C_{23}H_{37}N_9O_{14}P_2S\cdot 2H_2O$) C, H, N.

From the same column, the starting compounds **7** (6%) and **9** (5%) were separated. P^1,P^2-bis(3′-*C*-methyladenosine-5′-yl)pyrophosphate (**13**) as a white foam was also obtained (5%). ^{1}H NMR (D_2O): δ 1.50 (s, 3H, CH_3), 4.12 (m, 4H, H5′), 4.33 (m, 2H, H4′), 5.30 (d, J = 7.7 Hz, 2H, H2′), 6.10 (d, J = 7.32 Hz, 2H, H1′), 8.0 (s, 2H, H2), 8.20 (s, 2H, H8). ^{31}P NMR (D_2O): δ −11.08 (br s). MS m/z 703.2 $[MH]^-$. Anal. ($C_{22}H_{36}N_{12}O_{13}P_2\cdot 2H_2O$) C, H, N.

4.1.8. P^1-5′-[2-(β-D-ribofuranosyl)thiazole-4-carboxamide]-P^2-5′-[6-amino-9*H*-(3′-*C*-methyl-β-D-ribofuranosyl)-purine]pyrophosphate (2). Compound **11** was hydrolyzed as reported for **1** (120 mg, 0.16 mmol, reaction time 2.5 h). After purification, **2** as diammonium salt was lyophilized (88 mg, 81% yield). Compound purity by analytical HPLC was 97% (t_R = 6.4 min). ^{1}H NMR (D_2O): δ 1.40 (s, 3H, CH_3), 3.85–4.20 (m, 7H, H5′(3′-Me-A), H5′(T), H4′(3′-Me-A), H4′(T), H3′(T)), 4.90 (d, J = 4.9 Hz, 1H, H1′(T)), 5.35 (d, J = 7.6 Hz, 1H, H2′(3′-Me-A)), 6.10 (d, J = 7.6 Hz, 1H, H1′(3′-Me-A)), 7.80 (s, 1H, H5(T)), 8.02 (s, 1H, H2(3′-Me-A)), 8.38 (s, 1H, H8(3′-Me-A)). ^{31}P NMR (D_2O): δ −11.1 (br s). MS m/z 682.2 $[MH]^-$. Anal. ($C_{20}H_{33}N_9O_{14}P_2S\cdot 3H_2O$) C, H, N.

4.2. Biological methods

4.2.1. Expression and purification of human inosine 5′-monophosphate dehydrogenase (IMPDH), type I and type II. The coding region of IMPDH types I and II was cloned into pET23a (Novagen) expression vector and expressed in *E. coli* BL21 (DE3)pIMP strain.[21] Expression of IMPDH enzymes was induced by the addition of 1.0 mM IPTG. The enzymes were purified using a modification of the method described by Colby et al.[22] Briefly, induced cells were harvested and suspended at 4 °C in 50 mM Tris–HCl buffer, pH 8.0 containing 50 mM KCl, 2 mM EDTA, and 1 mM dithiothreitol. To the cell suspension, DNAase, RNAase, $MgCl_2$, and PMSF were added and lysed using French press. The lysate was centrifuged at 18,000*g* at 4 °C and filtered using a 0.45 mm filter. The filtrate was applied on to POROS HS1 cation exchange column using BIOCAD HPLC system and eluted with 0.1–1.0 M NaCl. IMPDH elutes as a single band at the start of a NaCl gradient. Active fractions were pooled, chilled to 4 °C and made up to 1 mM with dithiothreitol and loaded on to a Q-sepharose column equilibrated with 50 mM Tris–HCl buffer, pH 8.0 containing 50 mM KCl, 2 mM EDTA, and 1 mM dithiothreitol. IMPDH was eluted with a linear gradient of KCl buffer (0.05–1.0 M). All operations were carried out at 4 °C. Active fractions were pooled, concentrated, glycerol was added to 50% (v/v), and aliquots were stored at −70 °C until use for IMPDH kinetic studies.

4.2.2. Inosine 5′-monophosphate dehydrogenase assay and kinetic studies. The enzyme assay is based on a direct spectrophotometric analysis of NADH formed by the IMPDH reaction. The reaction mixture in a total volume of 1 mL contained 100 nmol IMP, NAD (20–100 nmol), 25 mM IMPDH tetramer, inhibitor (0.1–1.5 nmol) and assay buffer, 100 mM Tris–HCl, pH 8.0 containing 100 mM KCl, 2 mM EDTA, and 1 mM dithiothreitol. IMPDH was incubated with the inhibitor at 4 °C for 10 min before the addition of other ingredients and the reaction was started by the addition of NAD and the readings were recorded continuously within seconds up to 2 min at 37 °C using Genesys10 (Spectronic Unicam, Rochester, New York) at 340 nm. The enzyme activity was expressed as micromoles of NADH produced/min at 37 °C. Kinetic constants were calculated by using a computer program.[23] Kinetic values were established using Michaelis–Menten equation and inhibition constants were calculated from plots. A mean of three separate determinations are presented in Table 1.

4.2.3. Antitumor activity. Cytotoxicity of TAD and its analogues against human myelogenous leukemia K562/S cells was determined according to the cited methodology.[24] K562/S cells were maintained in RPMI 1640 medium containing 10% heat-inactivated fetal bovine serum. Logarithmically growing cells (0.1 mL; 5×10^4 cells/mL) were transferred into 96-well plates. After 24 h of initial incubation, cells were continuously treated for 72 h with appropriate concentration of the compounds (1.0–100.0 μM) prepared in saline and sterile filtered using 0.25 mm filter. At the end of 72 h tetrazolium reagent (20 mL) (Promega Corp., Madison, Wisconsin) was added and further incubated for 4 h and absorbance read at 490 nm using a microplate reader. Wells with serial dilutions of cells were utilized as control for the assay. In all cases controls indicated a linear response against cell number, with $R^2 \geqslant 0.99$.

TR resistant K562 cells were selected by subculturing sensitive K562 cells with subletal concentration of TR. After about 60 generations, cells were selected, which grew in the presence of 2 mM TR[25] at the same rate as the sensitive cells. Cells (2.5×10^4) were dispensed (0.1 mL) into 96 wells and incubated at 37 °C in an atmosphere of air and 5% carbon-di-oxide for 24 h. Various concentrations of the agents were added in triplicate and further incubated for 48 h. MTS reagent was added and absorbance at 490 nm was recorded.

4.2.4. Stability of T-2′-MeAD and T-3′-MeAD in culture medium. The stability of TAD analogues **1** and **2** was evaluated using 100 μM concentrations of T-2′-MeAD and T-3′-MeAD taken up in RPMI 1640 medium containing 10% heat-inactivated fetal bovine serum (Sigma Chemical Co.), and incubated for 0 min, 24, 48, and 72 h. Cold trichloroacetic acid (10%) was then added to precipitate the proteins. The mixture was kept on ice for 10 min and then centrifuged at 18,000*g* for 5 min in the cold. To the supernatant, 2 volumes of 0.5 M tri-*n*-octylamine in Freon were added, mixed thoroughly and centrifuged at 18,000*g* for 2 min. The aqueous layer was taken (top layer) and an aliquot analyzed on HPLC as described in general procedure. T-2′-MeAD and T-3′-MeAD were also analyzed without serum containing medium and found to be stable.

4.3. Computational chemistry

The program PCMODEL[26,27] was used to convert TAD from 1ADF into the different file formats required for input to the programs SPARTAN,[28–30] SYBYL,[31] and MACROMODEL.[32] As usual, the atom types and bond types had to be fixed after importing a molecule into the different computational chemistry programs in order that the most appropriate force field parameters are invoked. Unless otherwise noted, the default options were used in each program. PCMODEL was used to add a methyl group at the 2′ and 3′ positions to give analogues T-2′-MeAD and T-3′-MeAD. SPARTAN was used to energy minimize the structure using the Merck Molecular Force Field [MMFF94].[33–42] This force field is known to perform quite well for pharmaceutically related molecules.[43,44] Minimization finds the energy well closest to the starting conformation on the potential energy surface. Using the optimized structure, a systematic conformational search on each molecule was performed using SPARTAN and MMFF94. Molecular dynamics simulations trace the conformation of a molecule or set of molecules over a time course.[45,46] The simulations were started with the optimized structures, so all bond lengths and bond angles were initially at their equilibrium values. Our calculations were performed with a time step of 1 fs at a temperature of 300 K and a trajectory length

of 10,000 fs. After each simulation, the molecules were again minimized with the same force field to relax all geometrical variables. The MMFF94 force field was used in SYBYL and no solvation effect was included. The MMFF94 force field is not good enough to make the adenine exactly planar, but the geometry was roughly so. With MACROMODEL the MMFF94s force field was used for the unsolvated molecules as well as for the molecules solvated by implicit water.[47] The MMFF94s force field could make the adenine nearly planar, but the amino group was somewhat pyramidal. We used the superimposition algorithm in MACROMODEL to fit and measure the root mean square deviation (RMSD) between two molecules. The algorithm requires the same number of atoms and hence the $-CH_3$ group attached at 2′ and 3′ positions in the analogues were removed for running this fit. Except for hydrogen atoms in the $-NH_2$ and –OH groups, all other hydrogen atoms were deleted. Superimpositioning maximizes the overlap of paired atoms between two molecules. The RMSD values are reported in the figure captions.

Acknowledgements

The research was supported by the Italian MIUR (PRIN 2002), and by the Project Development Program, Research and Sponsored Programs, Indiana University, Indianapolis. We thank Prof. Massimo Bramucci for the stability assay and Dr. Kelsey Forsythe for management of the molecular modeling software and hardware at IUPUI.

References and notes

1. Franchetti, P.; Grifantini, M. *Curr. Med. Chem.* **1999**, *6*, 599–614, and references cited therein.
2. Konno, Y.; Natsumeda, Y.; Nagai, M.; Yamaji, Y.; Ohno, S.; Suzuki, K.; Weber, G. *J. Biol. Chem.* **1991**, *266*, 506–509.
3. Nagai, M.; Natsumeda, Y.; Konno, Y.; Hoffman, R.; Irino, S.; Weber, G. *Cancer Res.* **1991**, *51*, 3886–3890.
4. Nagai, M.; Natsumeda, Y.; Weber, G. *Cancer Res.* **1992**, *52*, 258–261.
5. Cooney, D. A.; Jayaram, H. N.; Gebeyehu, G.; Betts, C. R.; Kelley, J. A.; Marquez, V. E.; Johns, D. G. *Biochem. Pharmacol.* **1982**, *31*, 2311–2316.
6. Jayaram, H. N.; Ahluwalia, G. S.; Dion, R. L.; Gebeyehu, G.; Marquez, V. E.; Kelley, J. A.; Robins, R. K.; Cooney, D. A.; Johns, D. G. *Biochem. Pharmacol.* **1983**, *32*, 2633–2636.
7. Franchetti, P.; Cappellacci, L.; Perlini, P.; Jayaram, H. N.; Butler, A.; Schneider, B. P.; Collart, F. R.; Huberman, E.; Grifantini, M. *J. Med. Chem.* **1998**, *41*, 1702–1707.
8. Goldstein, B. M.; Colby, T. D. *Curr. Med. Chem.* **1999**, *6*, 519–536, and references cited therein.
9. Ong, S. P.; McFarlan, S. C.; Hogenkamp, H. P. C. *Biochemistry* **1993**, *32*, 11397–11404.
10. Franchetti, P.; Cappellacci, L.; Marchetti, S.; Trincavelli, T.; Martini, C.; Mazzoni, M. R.; Lucacchini, A.; Grifantini, M. *J. Med. Chem.* **1998**, *41*, 1708–1715.
11. Ong, S. P.; Nelson, L. S.; Hogenkamp, H. P. C. *Biochemistry* **1992**, *31*, 11210–11215.
12. Gebeyehu, G.; Marquez, V. E.; Kelley, J. A.; Cooney, D. A.; Jayaram, H. N.; Johns, D. G. *J. Med. Chem.* **1983**, *26*, 922–925.
13. Zatorski, A.; Goldstein, B. M.; Colby, T. D.; Jones, J. P.; Pankiewicz, K. W. *J. Med. Chem.* **1995**, *38*, 1098–1105.
14. Leach, A. R. In *Reviews in Computational Chemistry*; Lipkowitz, K. B., Boyd, D. B., Eds.; VCH: New York, 1991; Vol. 2, pp 1–55.
15. Leach, A. R. *Molecular Modeling: Principles and Applications*, 2nd ed.; Pearson Education: Harlow, UK, 2001.
16. Boyd, D. B. *Ullmann's Encyclopedia of Industrial Chemistry*, 6th ed.; Wiley-VCH: Weinheim, 1998, on CD-ROM.
17. Berman, H. M.; Westbrook, J.; Feng, Z.; Gilliland, G.; Bhat, T. N.; Weissig, H.; Shindyalov, I. N.; Bourne, P. E. *Nucleic Acids Res.* **2000**, *28*, 235–242.
18. Li, H.; Hallows, W. H.; Punzi, J. S.; Marquez, V. E.; Carrell, H. L.; Pankiewicz, K. W.; Watanabe, K. A.; Goldstein, B. M. *Biochemistry* **1994**, *33*, 23–32.
19. See, for example, Liljefors, T.; Gundertofte, K.; Norrby, P.-O.; Pettersson, I. In *Computation Medicinal Chemistry for Drug Discovery*; Bultinck, P., Winter, H., Langenaeker, W., Tollenaere, J. P., Eds.; Marcel Dekker: New York, 2004; pp 1–28; Boyd, D. B. In *The Amide Linkage: Structural Significance in Chemistry, Biochemistry, and Materials Science*; Greenberg, A., Breneman, C. M., Liebman, J. F., Eds.; Wiley: New York, 2000; pp 337–375, and references cited therein.
20. Franchetti, P.; Cappellacci, L.; Pasqualini, M.; Petrelli, R.; Vita, P.; Jayaram, H. N.; Horvath, Z.; Szekeres, T.; Grifantini, M., in preparation.
21. Xiang, B.; Taylor, J. C.; Markham, G. D. *J. Biol. Chem.* **1996**, *271*, 1435–1440.
22. Colby, T. D.; Vanderveen, K.; Strickler, M. D.; Markham, G. D.; Goldstein, B. M. *Proc. Natl. Acad. Sci. U.S.A.* **1999**, *96*, 3531–3536.
23. Cleland, W. W. *Methods Enzymol.* **1979**, *63*, 103–138.
24. Yalowitz, J. A.; Pankiewicz, K. W.; Patterson, S. E.; Jayaram, H. N. *Cancer Lett.* **2002**, *181*, 31–38.
25. Jayaram, H. N.; Zhen, W.; Gharehbaghi, K. *Cancer Res.* **1993**, *53*, 2344–2348.
26. PCMODEL 8.5. Serena Software, Bloomington, Indiana 47402. http://www.serenasoft.com.
27. Schlecht, M. F. *Molecular Modeling on the PC*; Wiley: Hoboken, NJ, 1998.
28. Spartan '04. Wavefunction, Inc., Irvine, California 92612. http://www.wavefun.com.
29. Hehre, W. J.; Shusterman, A. J.; Nelson, J. E. *The Molecular Modeling Workbook for Organic Chemistry*; Wavefunction: Irvine, California, 1998.
30. Hehre, W. J. *A Guide to Molecular Mechanics and Quantum Chemical Calculations*; Wavefunction, Inc.: Irvine, California, 2003.
31. SYBYL® 6.9.2. Tripos Inc., 1699 South Hanley Rd., St. Louis, Missouri 63144. http://www.tripos.com.
32. Mohamadi, F.; Richards, N. G. J.; Guida, W. C.; Liskamp, R.; Lipton, M.; Caufield, C.; Chang, G.; Hendrickson, T.; Still, W. C. *J. Comput. Chem.* **1990**, *11*, 440–467.
33. Halgren, T. A. *J. Comput. Chem.* **1996**, *17*, 490–519.
34. Halgren, T. A. *J. Comput. Chem.* **1996**, *17*, 520–552.
35. Halgren, T. A. *J. Comput. Chem.* **1996**, *17*, 553–586.
36. Halgren, T. A.; Nachbar, R. B. *J. Comput. Chem.* **1996**, *17*, 587–615.
37. Halgren, T. A. *J. Comput. Chem.* **1996**, *17*, 616–641.
38. Halgren, T. A. *J. Comput. Chem.* **1999**, *20*, 720–729.
39. Halgren, T. A. *J. Comput. Chem.* **1999**, *20*, 730–748.
40. Halgren, T. A.; Bush, B. L. *Book of Abstracts*, 212th ACS National Meeting, Orlando, FL, Aug 25–29, 1996; COMP 002.

41. Halgren, T. A.; Nachbar, R. B. *Book of Abstracts*, 211th ACS National Meeting, New Orleans, LA, Mar 24–28, 1996; COMP 070.
42. Halgren, T. A. *Book of Abstracts*, 216th ACS National Meeting, Boston, MA, Aug 23–27, 1998; COMP 061.
43. Pettersson, I.; Liljefors, T. In *Reviews in Computational Chemistry*; Lipkowitz, K. B., Boyd, D. B., Eds.; VCH: New York, 1996; Vol. 9, pp 167–189.
44. Ercanli, T.; Boyd, D. B. 36th Central Regional Meeting of the American Chemical Society, Indiana University–Purdue University at Indianapolis, Indianapolis, Indiana, Jun 2–4, 2004.
45. Lybrand, T. P. In *Reviews in Computational Chemistry*; Lipkowitz, K. B., Boyd, D. B., Eds.; VCH: New York, 1990; Vol. 1, pp 295–320.
46. Boyd, D. B. In *Encyclopedia of Library and Information Science*; Kent, A., Ed.; Marcel Dekker: New York, 1997; Vol. 59, Suppl. 22, pp 54–84.
47. Cramer, C. J.; Truhlar, D. G. In *Reviews in Computational Chemistry*; Lipkowitz, K. B., Boyd, D. B., Eds.; VCH: New York, 1995; Vol. 6, pp 1–72.